Supporting Information

Intense Visible and Near-Infrared Upconversion Photoluminescence in Colloidal $LiYF_4:Er^{3+}$ Nanocrystals under Laser Excitation of 1490 nm

*Guanying Chen, [†‡] Tymish Y. Ohulchanskyy, [†] Aliaksandr Kachynski, [†] Hans Ågren, [‡] and Paras N. Prasad[†]**

[†]*Institute for Lasers, Photonics, and Biophotonics, The State University of New York, University at Buffalo, Buffalo, New York 14260*

[‡]*Department of Theoretical Chemistry, Royal Institute of Technology, S-10691 Stockholm, Sweden*

*Corresponding Author. E-mail: pnprasad@buffalo.edu

Contents:

I. Supporting Images

1. HRTEM micrograph

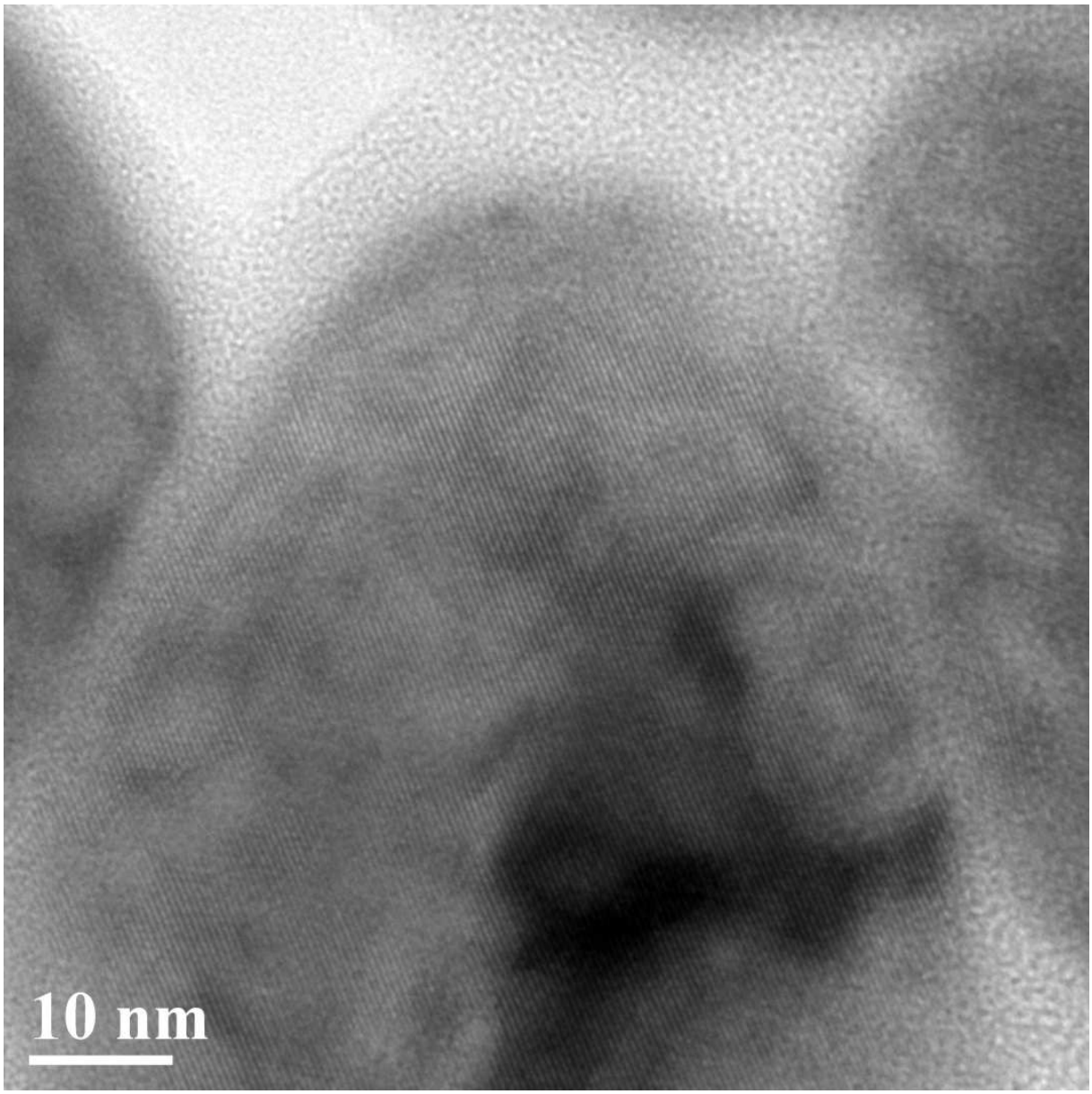

Figure S1. A high-resolution transmission microscopy (HRTEM) image of the individual $LiYF_4:Er^{3+}$ nanocrystal, displaying the lattice fringes.

2. Photographic images of upconversion photoluminescence under unfocused laser excitation

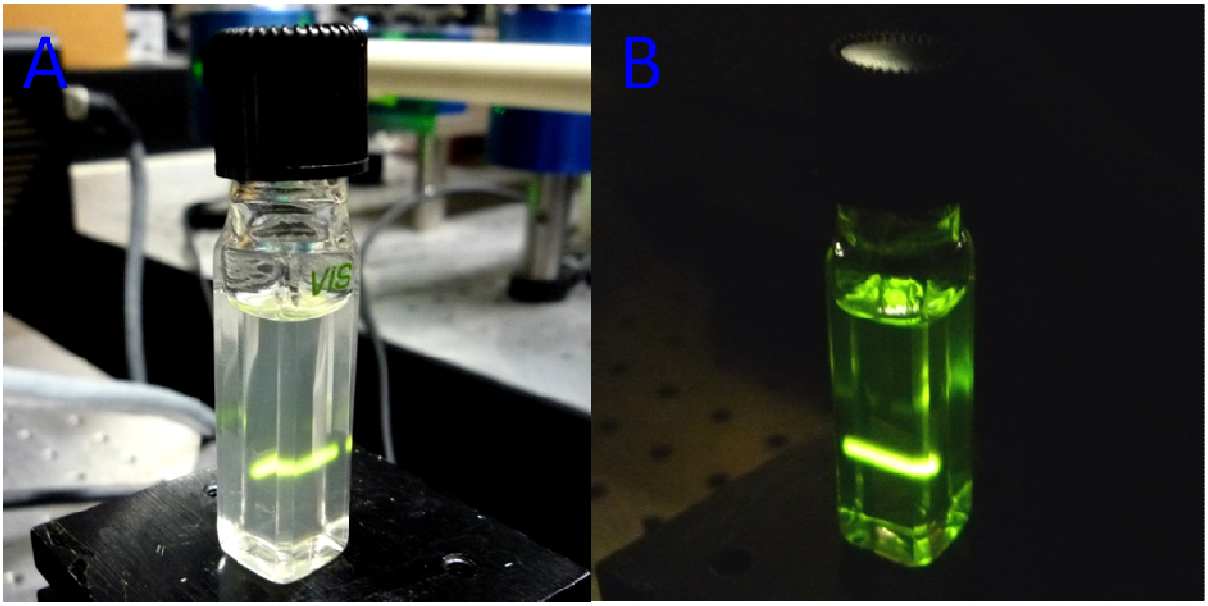

Figure S2. Digital images of colloidal $LiYF_4:Er^{3+}$ 10% nanocrystals in chloroform (1% wt) via unfocused 1490 nm laser excitation with 4 W/cm^2 under (a) daylight and (b) reduced background illumination.

II. Determination of Upconversion Photoluminescence Quantum Yield

1. Principle of UCQY determination

The upconversion quantum yield (UCQY) is defined as the ratio of the number of the emitted upconverted photons to the number of the absorbed NIR photons, according to the following formula,

$$UCQY = \frac{Photons\ Emitted}{Photons\ Absorbed} = \frac{E}{A} \quad \text{(S1)}$$

Only few works on measurements of the quantum yield of multiphoton upconversion emission were reported up to date. Here, we have determined the UCQY of our particles using the core/shell ($NaYF_4$:Yb^{3+}20%, Er^{3+}2%)/$NaYF_4$ nanocrystals with known UCQY as a reference. The following equations (S2) and (S3) describe the quantum yield of samples to be measured and referenced:

$$UCQY_S = \frac{E_S}{A_S} \quad , \quad \text{(S2)}$$

$$UCQY_R = \frac{E_R}{A_R}, \quad \text{(S3)}$$

where $UCQY_S$ and $UCQY_R$ are the upconversion quantum yield of the sample to be determined and reference sample, respectively; E_S and E_R are the numbers of the emitted photons for measured sample and reference sample, respectively; and A_S and A_R are the numbers of the photons absorbed by measured sample and referenced sample, respectively. According to equations (S2) and (S3), the $UCQY_S$ of the sample to be determined:

$$UCQY_S = \left(\frac{E_S}{E_R}\right)\left(\frac{A_R}{A_S}\right)UCQY_R \quad \text{(S4)}$$

As can be seen in Equation (S4), the UCQY of the measured sample can be determined by the measurements of the upconversion photoluminescence (PL) intensities and the absorption values at the excitation wavelengths for the measured sample and the reference sample, since the value of $UCQY_R$ is already known.

2. Reference sample

The absolute quantum yield measurements of the most efficient colloidal $NaYF_4:Er^{3+}/Yb^{3+}$ upconversion nanoparticles has recently been reported by Boyer et al [Ref. 36, *Nanoscale* **2**, 1417 (2010)]. We use ~30 nm sized $(NaYF_4:20\%Yb^{3+}/2\%Er^{3+})/NaYF_4$ core/shell nanocrystals as the reference sample, which has a reported quantum yield of 0.3% for the green emission under ~980 nm excitation with 150 W/cm^2. This quantum yield is the same as that for 100 nm sized $NaYF_4:20\%Yb^{3+}/2\%Er^{3+}$ nanocrystals.[36] The ~ 30 nm sized $(NaYF_4:20\%Yb^{3+}/2\%Er^{3+})/NaYF_4$ core/shell nanoparticle sample was synthesized using exactly the same synthetic procedure outlined in the Ref. 36 and in its cited reference [Ref. S1, *Langmuir*, **24**, 12123 (2008)]. No changes were made to the reported procedures.

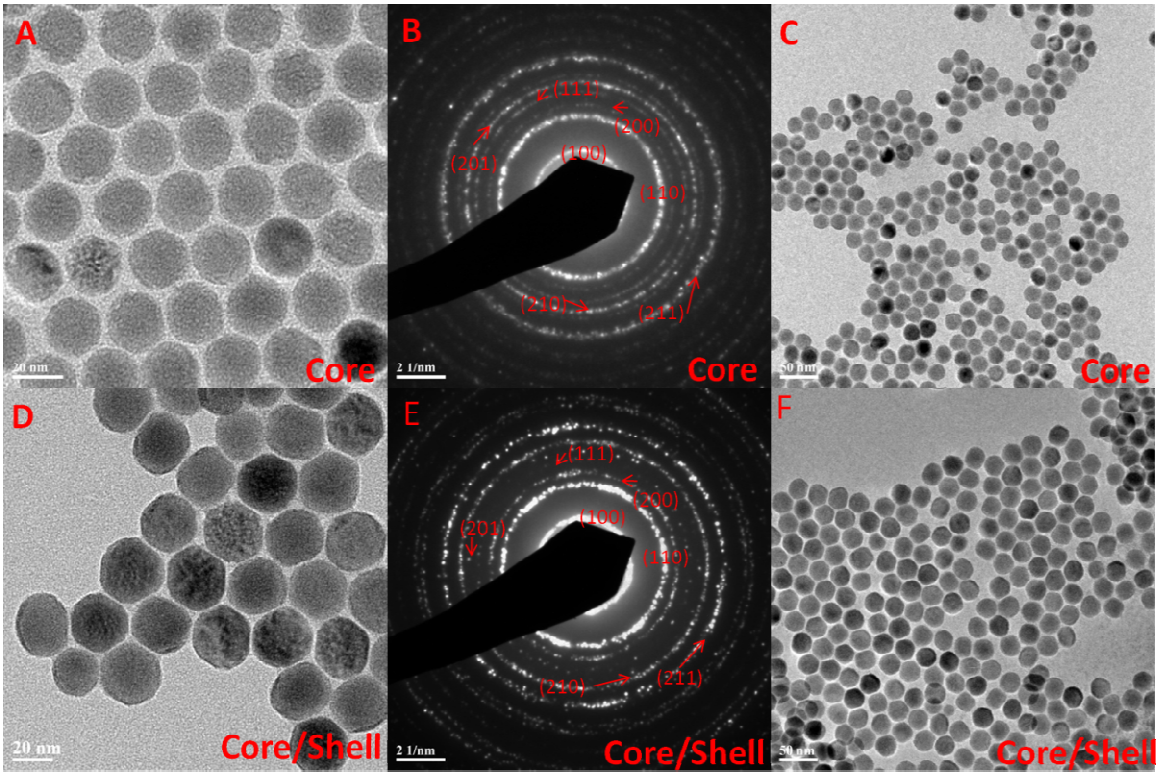

Figure S3. Transmission electron images of (A, C) $NaYF_4:20\%Yb^{3+}/2\%Er^{3+}$ core and (D, F) $(NaYF_4:20\%Yb^{3+}/2\%Er^{3+})/NaYF_4$ core/shell powders displaying the size of these particles. Selected area electron diffraction patterns of (B) $NaYF_4:20\%Yb^{3+}/2\%Er^{3+}$ core and of (D) $(NaYF_4:20\%Yb^{3+}/2\%Er^{3+})/NaYF_4$ core/shell particles. As shown in Figure S2, the size of the $NaYF_4:20\%Yb^{3+}/2\%Er^{3+}$ core is about ~20 nm, and the size of the core/shell

(NaYF4:20%Yb^{3+}/2%Er^{3+})/$NaYF_4$ nanoparticles is about ~30 nm, agreeing well with that in Ref. 36 and Ref. S1. The selected area transmission electron diffraction patterns in Figure S3(B) and (E) confirm that they are of both hexagonal structure, and can be indexed to the JCPDS 28-1192 hexagonal $NaYF_4$ structure.

3. Measurement of the upconversion quantum yield

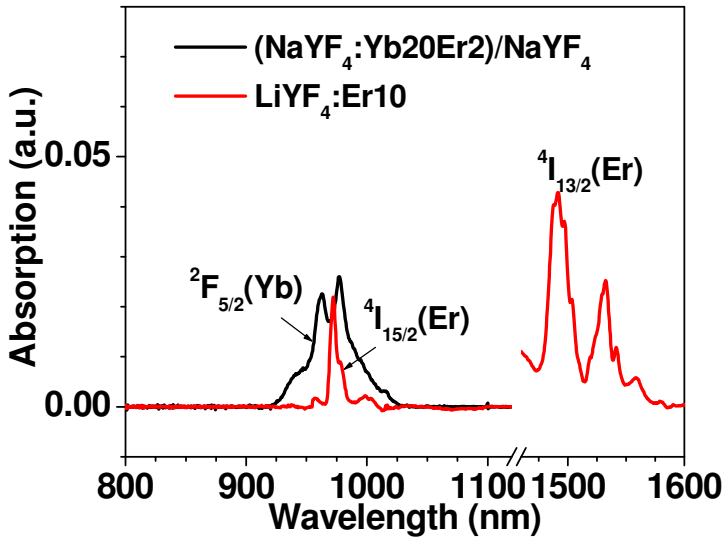

Figure S4. The absorption spectra of colloidal $LiYF_4$:Er^{3+} 10% nanocrystals and the core/shell (NaYF4:20%Yb^{3+}/2%Er^{3+})/$NaYF_4$ nanocrystals. Absorptions at 971 nm have been normalized by adjusting the concentration of these two samples. As both the laser excitation of 971 nm and 1490 nm was provided by the same tunable optical parametric oscillator with a line width of only 0.4 nm, the peak value at 971 nm and 1490 nm was used to determine the parameter of A_R/A_S in equation (S4), which was calculated to be about 0.5.

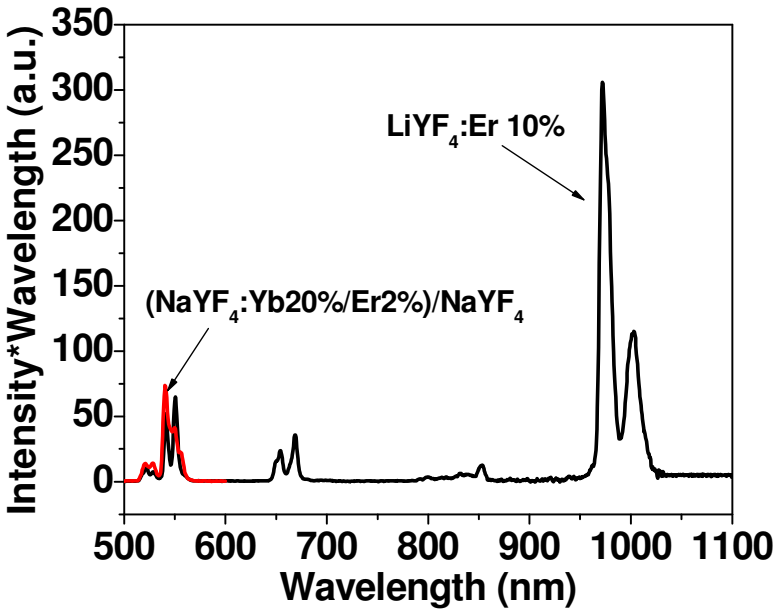

Figure S5. Upconversion PL of colloidal $LiYF_4:Er^{3+}$% nanocrystals under 1490 nm excitation with 150 W/cm^2 (black), as well as the green emission of colloidal ($NaYF_4$:20%Yb^{3+}/2%Er^{3+})/$NaYF_4$ core/shell nanocrystals under 971 nm excitation with 150 W/cm^2 (red). We emphasize that the same optical geometry was used in the experiment to obtain spectra shown in Figure S5, since the excitation at 971 nm and 1490 nm were from the same tunable optical parametric oscillator, and the same laser power was used, adjusted with a neutral density filter. The measurements were repeated using three different concentrations of our sample and referenced core/shell $NaYF_4$:20%Yb^{3+}/2%Er^{3+})/$NaYF_4$ nanocrystals. The intensities of three-photon green emission peaked at 540 nm, three-photon red emission peaked at 660 nm, and two-photon NIR emission peaked at 800 and 970 nm in $LiYF_4:Er^{3+}$ 10% nanocrystals were found to be about 0.85±0.10, 0.50±0.10, 0.34±0.10, 6.3±0.3 times of the intensity of green emission in ($NaYF_4$:20%Yb^{3+}/2%Er^{3+})/$NaYF_4$ core/shell nanocrystals. According to equation (S4), this corresponds to a UCQY of 0.13±0.02%, 0.07±0.02%, 0.05±0.01%, and 0.95±0.05%, for the emissions at 540, 660, 800, and 970 nm, respectively. Hence, a total upconversion photoluminescence quantum yield of $LiYF_4:Er^{3+}$ 10% nanocrystals under 1490 nm excitation is 1.2±0.1%; this value is almost four times higher than the UCQY of 0.3% reported for 100 nm sized $NaYF_4$:20%Yb^{3+}/2%Er^{3+} nanocrystals.

III. Additional Supporting Figures

1. Normalized photoluminescence spectra

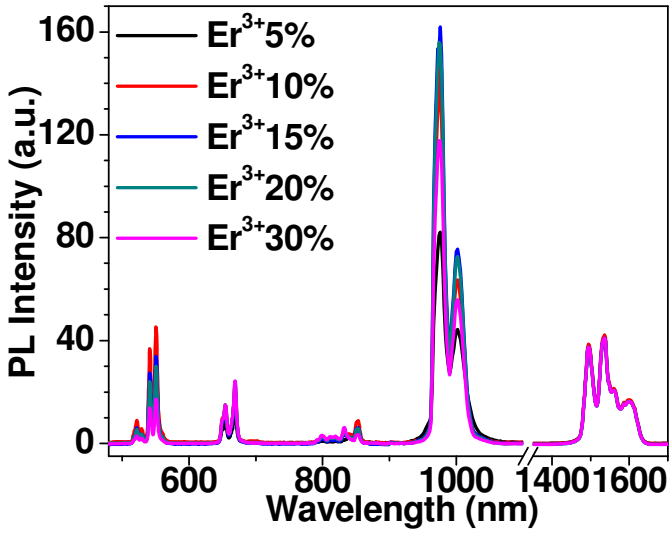

Figure S6. PL spectra of colloidal $LiYF_4$ nanocrystals doped with 5, 10, 15, 20, and 30% Er^{3+} ions under laser excitation at 1490 nm. Spectra were normalized for Er^{3+} emission at 1494 nm.

2. Dependence of photoluminescence intensity on the excitation power density in the range of ~0.3-4.5W/cm^2

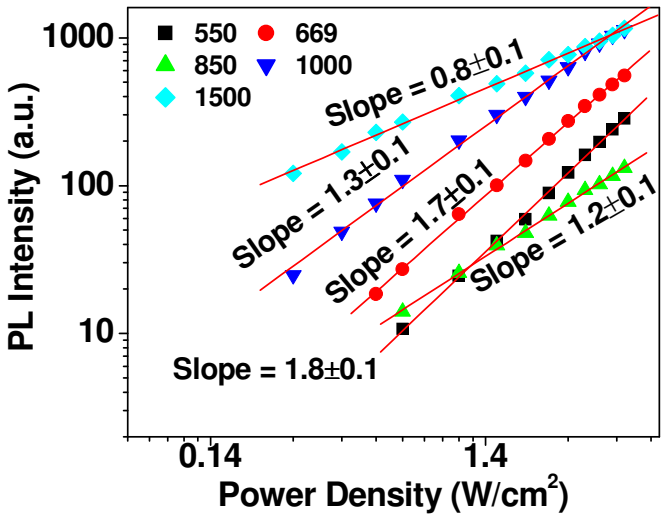

Figure S7. The dependence of the intensities of all PL bands of colloidal $LiYF_4$:10% Er^{3+}

nanocrystals on the power of excitation at 1490 nm under lower power density (~0.3-4.5 W/cm^2). As one can see, a slope value of 1.7 and 1.8 is observed for three-photon red emission at 650 nm and green emission at 550 nm; these slope values are higher than those of 0.9 and 1.0 for the power density range of 5-120 W/cm^2 (Figure 3). Two-photon radiations at 800 and 1000 nm have slope values of 1.2 and 1.3, which are higher than values of 0.8 in Figure 3 in the power density range of 5-120 W/cm^2. In addition, the same slope value of 0.8 is observed for the Stokes one-photon emission at 1500 nm as that in Figure 3. These results show that three- and two-photon upconversion emissions for the excitation power density range of 0.24-5 W/cm^2 are still saturated to some extent. Otherwise, if there is no saturation, the slopes values would be 3 and 2, correspondingly.

3. Photoluminescence decay profiles

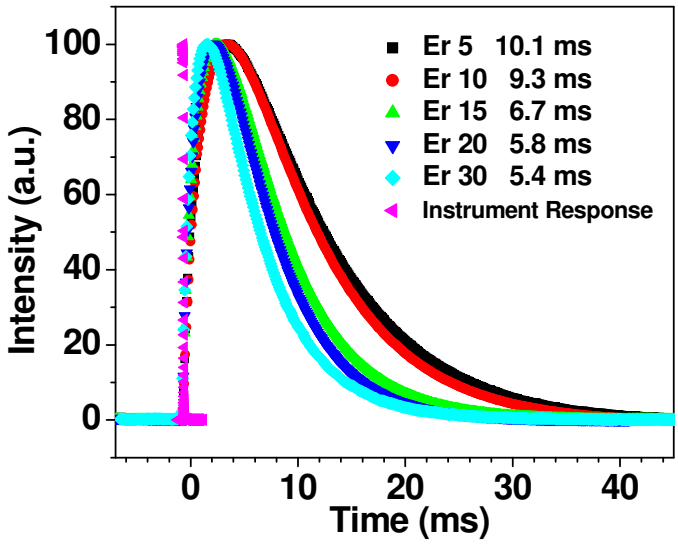

Figure S8. Decays of PL at 1535 nm (corresponding to the $^4I_{13/2} \rightarrow {}^4I_{15/2}$ transition) for colloidal $LiYF_4$ nanocrystals doped with 5, 10, 15, 20, and 30% Er^{3+} ions. The rising stage in the PL decay is due to the fact that the $^4I_{13/2}$ state is populated by relaxations from the $^4I_{11/2}$ state which is

directly excited by laser. As the $^4I_{11/2}$ state has a long lifetime of about 2 ms (see Figure S8), the decay trace of the $^4I_{13/2}$ state is delayed by such a time range, in good agreement with the observation in Figure S7. Nanocrystals of $LiYF_4$ doped with 5% and 10% Er^{3+} ions have an average PL lifetime of ~10.1 and 9.4 ms, respectively. The similar lifetime values indicate inefficient concentration quenching effect for Er^{3+} ion concentration less than 10%. The PL lifetime decreases rapidly from 9.4 ms to 6.7 ms when Er^{3+} ions increases from 10% to 15%, which might illustrate that a concentration quenching effect begins due to the formation of Er^{3+} ion clusters in the lattice for Er^{3+} ion concentration of 15%. The PL lifetime then gradually becomes shorter (decreasing from 6.7 ms to 5.4 ms) for $LiYF_4$ nanocrystals with the increase in relative content of Er^{3+} ions from 15% to 30%.

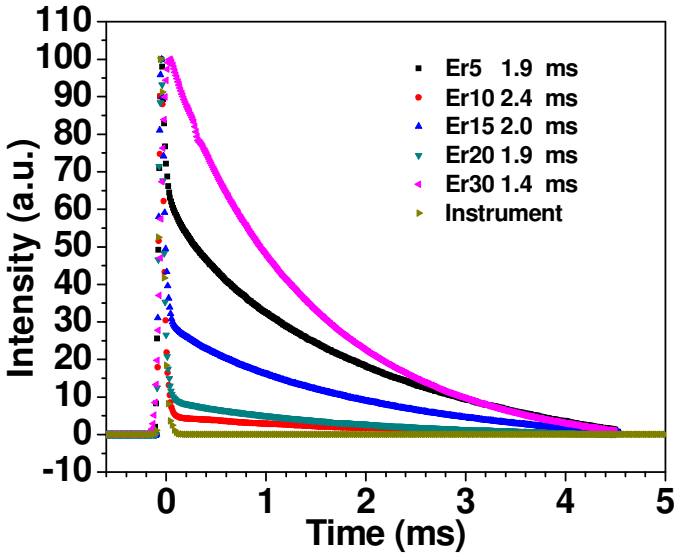

Figure S9. Decays of PL at 1005 nm (corresponding to the $^4I_{11/2} \rightarrow {}^4I_{15/2}$ transition) for colloidal $LiYF_4$ nanocrystals doped with 5, 10, 15, 20, and 30% Er^{3+} ions. Unlike PL decay at 1535 nm, the lifetime at first increases from 1.9 to 2.4 ms with an increase in the Er^{3+} ions concentration from 5% to 10%. As there is a negligible quenching effect in this range, the small increase in

lifetime might be induced by the "photon trapping" effect giving rise to apparent longer experimental lifetime, as observed for other ions, e.g., Yb^{3+}.[S2] A sharp decrease of PL lifetime from 2.4 to 2.0 ms, similar to the PL decay at 1550 nm, is also apparently arised from the formation of Er^{3+} ion clusters at ion concentration of 15%. Then, the PL lifetime gradually becomes shorter (decreasing from 2.0 ms to 1.5 ms) for $LiYF_4$ nanocrystals due to a gradual increase of cluster concentrations along with the increment of Er^{3+} ions from 15% to 30%.

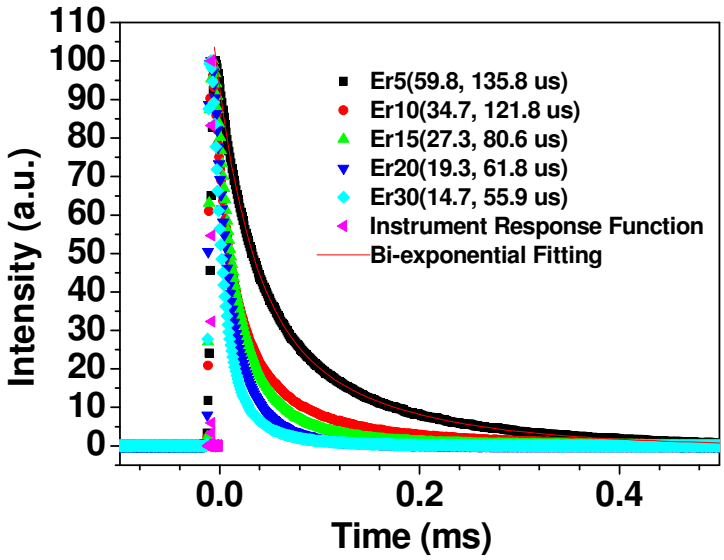

Figure S10. Decays of PL at 548 nm (corresponding to the $^2H_{11/2}/^4I_{13/2} \rightarrow {}^4I_{15/2}$ transition) under excitation with 532 nm for $LiYF_4$ nanocrystals doped with Er^{3+} of 5, 10, 15, 20, and 30%. As shown in the Figure, the decay traces of 548 nm can be well fitted by bi-exponential decays. This is due to the involvement of two upper states, the $^2H_{11/2}$ state the $^4S_{3/2}$ state, which correspond to a short and a long lifetime, respectively.[11b,c] The lifetime of the $^2H_{11/2}$ and $^4S_{3/2}$ states were estimated to vary in the range of 15-60 μs and 56-136 μs, respectively.

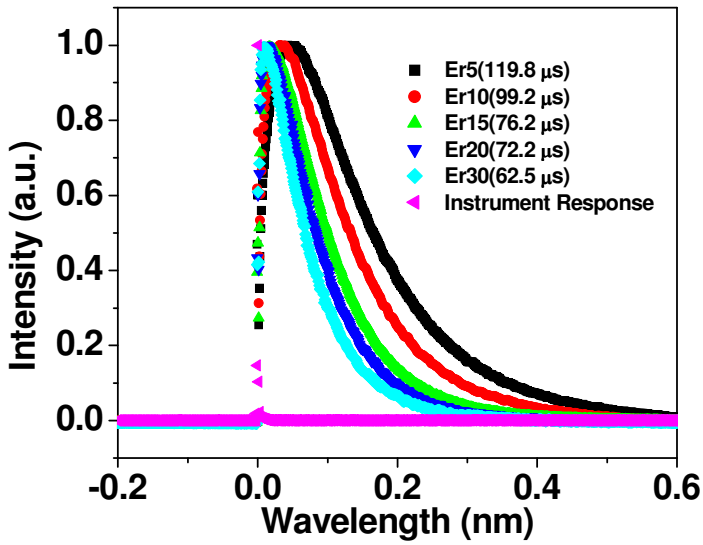

Figure S11. Decays of PL at 667 nm (corresponding to the $^4F_{9/2} \rightarrow {}^4I_{15/2}$ transition) for nanocrystals $LiYF_4$ nanocrystals doped with Er^{3+} of 5, 10, 15, 20, and 30%. The lifetime of the $^4F_{9/2}$ state was evaluated to be 63-120 μs in Figure S10.

In conclusion, the lifetime of intermediate states is extremely long, e.g., 5.4-10 ms for the $^4I_{13/2}$ state and 1.5-2.4 ms for the $^4I_{11/2}$ state. In contrast, the higher emitting states have much shorter lifetimes, e.g., the $^4F_{9/2}$ state of 63-120 μs and the $^4S_{3/2}$ state of 56-136μs. These data clearly support our conclusion that the long lifetime intermediate states are of importance in our system due to their reservoir capability, resulting in the efficient upconversion process.

Supporting References

S1. Qian, H.; Zhang, Y. Synthesis of Hexagonal-Phase Core-Shell $NaYF_4$ Nanocrystals with Tunable Upconversion Fluorescence. *Langmuir*, **2008**, *24*, 12123—12125.

S2. Auzel, F. Upconversion and Anti-Stokes Processes with f and d Ions in Solids. *Chem. Rev.* **2004**, *104*, 139—173.